Journal of Molecular Catalysis A: Chemical 334 (2011) 103–107

Contents lists available at ScienceDirect

Journal of Molecular Catalysis A: Chemical

journal homepage: www.elsevier.com/locate/molcata

# Microstructure control of magnesium dichloride crystallites by electron donors: The effect of methanol

Anniina Turunen[a], Mikko Linnolahti[a,*], Virve A. Karttunen[a], Tapani A. Pakkanen[a,*], Peter Denifl[b], Timo Leinonen[b]

[a] Department of Chemistry, University of Eastern Finland, P.O. Box 111, FI-80101 Joensuu Campus, Finland
[b] Borealis Polymers Oy, R&D, P.O. Box 330, FI-06101 Porvoo, Finland

ARTICLE INFO

*Article history:*
Received 11 June 2010
Received in revised form 3 November 2010
Accepted 8 November 2010
Available online 13 November 2010

*Keywords:*
Ziegler–Natta
Computational catalysis
Electron donors

ABSTRACT

The ability to control the microstructure of magnesium dichloride ($MgCl_2$) crystallites by electron donors was demonstrated by quantum chemical calculations, using methanol as a model donor. Investigation of sets of differently shaped $MgCl_2$ crystallites showed the dominance of the five-fold coordinated (1 0 0) crystal surface over the four-fold coordinated (1 1 0) surface to emerge as a factor increasing crystallite stability. To study the role of electron donors in controlling $MgCl_2$ crystallite shape, crystallites were saturated with methanol. The stability order of the crystallites was significantly affected by donor adsorption. Reverse to the case of pure $MgCl_2$, crystallites with the highest (1 1 0) to (1 0 0) surface site ratio became the most stable after donor adsorption. This indicates control of the shape of $MgCl_2$ crystallites to be attainable by appropriate choice of electron donor, a result utilizable in heterogeneous Ziegler–Natta olefin polymerization catalysis.



## 1. Introduction

Magnesium dichloride is a key component in heterogeneous Ziegler–Natta olefin polymerization catalysis with the role of acting as a support material into which transition metal complexes, typically titanium chloride, are bound, thereby generating catalytically active sites [1–4]. The reactive sites of $MgCl_2$ are the coordinatively unsaturated edges [5], in particular, the (1 0 0) surface with five-coordinate Mg and the (1 1 0) surface with four-coordinate Mg (Fig. 1) [6,7]. The two unsaturated surfaces differ in their binding abilities due to the different coordinative saturation and steric environment [8–17]. FT-Raman measurements indicate that (1 1 0) is the preferred lateral cut for binding of titanium chloride [18,19].

In addition to titanium chloride, various additives are often included into the catalyst system to optimize the catalytic performance. Electron donor compounds comprise a frequently used class of such additives. The traditional role of the donor compounds has been to act as an agent increasing the stereospecificity and activity of the catalyst. Other advantages gained from the use of donors include better control over the properties of the polymerization product, such as polymer yield and molecular weight [20–25]. Recently, $MgCl_2$ crystal structures have been regulated by electron donors. The results indicate that inclusion of a suitable donor in the crystallite preparation process leads to the exclusive formation of merely one $MgCl_2$ surface type, i.e. either the (1 0 0) or the (1 1 0) surface on the crystallite edges. Without the addition of donors, both surface types are present in the prepared crystallites [26–30]. Similar regulation of the crystal structure has been reported also for other compounds, such as $CaCO_3$ [31] and $TiO_2$ [32].

The role of the electron donors in affecting the polymerization behaviour of the $MgCl_2/TiCl_4$ catalytic system is not fully understood. Electron donors have been proposed to have either a direct influence on stereoselectivity by binding to the active Ti centers [33], or an indirect influence through binding to the $MgCl_2$ surface in the vicinity of the active sites. A donor binding to the more reactive (1 1 0) surface is likely to affect the stereospecificity by hindering the formation of aspecific mononuclear Ti centers, whereas donor binding to the (1 0 0) surface likewise hinders the formation of stereospecific dinuclear Ti centers [34,35]. Various modes of binding to the $MgCl_2$ surface are viable for the donors [36], complicating the study, but enhancing the different preferences for binding to either (1 1 0) or (1 0 0) surface, thereby affecting both the structure and the properties of the catalytic system.

The focus of the theoretical study reported herein is on the microstructure regulation of $MgCl_2$ crystallites, with ultimate motivation on control of the catalytic behaviour through control the relative proportion of (1 0 0) and (1 1 0) surface sites. Sets of differently shaped and sized $(MgCl_2)_n$ crystallites are studied in order

* Corresponding authors. Tel.: +358 13 251 3345; fax: +358 13 251 3344.
*E-mail addresses:* mikko.linnolahti@uef.fi (M. Linnolahti), tapani.pakkanen@uef.fi (T.A. Pakkanen).

1381-1169/$ – see front matter © 2010 Elsevier B.V. All rights reserved.
doi:10.1016/j.molcata.2010.11.003

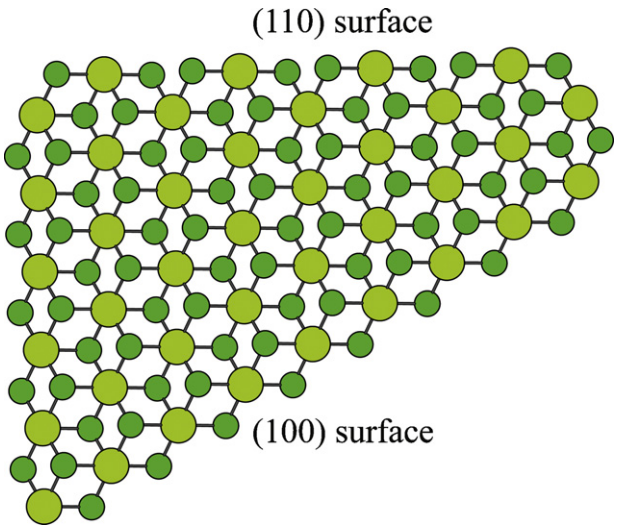


**Fig. 1.** The (1 0 0) and (1 1 0) lateral cuts of $MgCl_2$.

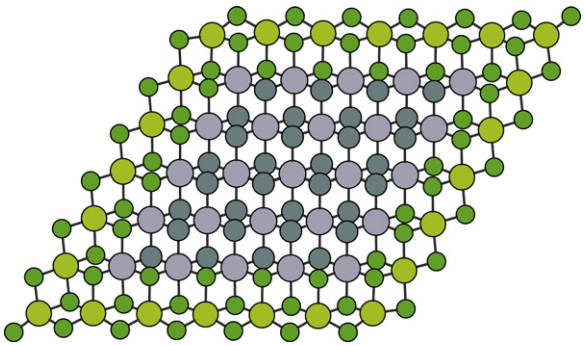

**Fig. 2.** Optimization of the $Mg_{49}Cl_{98}$ quadrangle-shaped crystallite. Gray atoms were fixed to the β-$MgCl_2$ crystal lattice, green and yellow atoms were relaxed. (For interpretation of the references to color in this figure legend, the reader is referred to the web version of the article.)

to establish the effects on crystallite stability, with a particular emphasis on examining the differences arising from different proportions of (1 0 0) and (1 1 0) surface sites on the crystallite edges. The crystallites are then saturated with methanol, used as a model

| Shape | Initial structure | Enlarged model | Models in the set |
|---|---|---|---|
| Quadrangles | 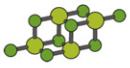 | 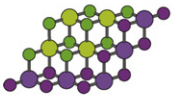 | $Mg_4Cl_8$, $Mg_9Cl_{18}$, $Mg_{16}Cl_{32}$, $Mg_{25}Cl_{50}$, $Mg_{36}Cl_{72}$, $Mg_{49}Cl_{98}$, $Mg_{64}Cl_{128}$, $Mg_{81}Cl_{162}$ |
| Hexagons | 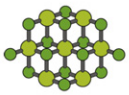 | 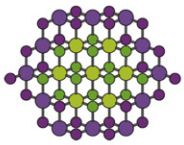 | $Mg_7Cl_{14}$, $Mg_{19}Cl_{38}$, $Mg_{37}Cl_{74}$, $Mg_{61}Cl_{122}$, $Mg_{91}Cl_{182}$ |
| Diamonds | 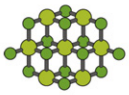 | 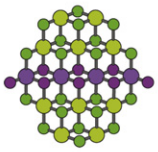 | $Mg_7Cl_{14}$, $Mg_{14}Cl_{28}$, $Mg_{23}Cl_{46}$, $Mg_{34}Cl_{68}$, $Mg_{47}Cl_{94}$, $Mg_{62}Cl_{124}$, $Mg_{79}Cl_{158}$ |
| Pyramids | 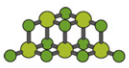 | 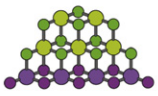 | $Mg_5Cl_{10}$, $Mg_9Cl_{18}$, $Mg_{14}Cl_{28}$, $Mg_{20}Cl_{40}$, $Mg_{27}Cl_{54}$, $Mg_{35}Cl_{70}$, $Mg_{44}Cl_{88}$, $Mg_{54}Cl_{108}$, $Mg_{65}Cl_{130}$, $Mg_{77}Cl_{154}$ |
| Triangles | 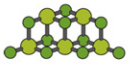 | 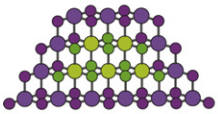 | $Mg_5Cl_{10}$, $Mg_{18}Cl_{36}$, $Mg_{39}Cl_{78}$, $Mg_{68}Cl_{136}$ |
| (110) slabs | 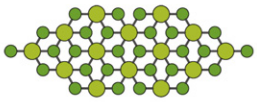 | 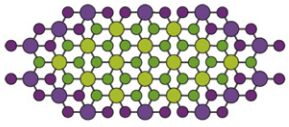 | $Mg_{14}Cl_{28}$, $Mg_{28}Cl_{56}$, $Mg_{46}Cl_{92}$, $Mg_{68}Cl_{136}$, $Mg_{94}Cl_{188}$ |
| (110) pipes | 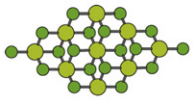 | 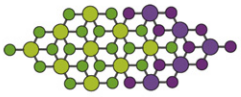 | $Mg_9Cl_{18}$, $Mg_{14}Cl_{28}$, $Mg_{19}Cl_{38}$, $Mg_{24}Cl_{48}$, $Mg_{29}Cl_{58}$, $Mg_{34}Cl_{68}$, $Mg_{39}Cl_{78}$, $Mg_{44}Cl_{88}$, $Mg_{54}Cl_{108}$, $Mg_{64}Cl_{128}$, $Mg_{74}Cl_{148}$, $Mg_{84}Cl_{168}$, $Mg_{94}Cl_{188}$, $Mg_{104}Cl_{208}$ |

**Fig. 3.** The $(MgCl_2)_n$ crystallite model sets and their construction principles.

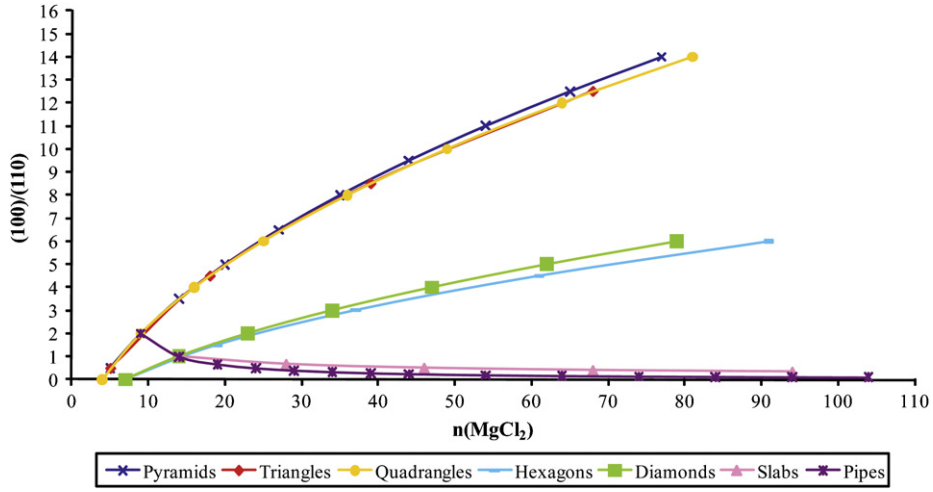


**Fig. 4.** The (1 0 0) to (1 1 0) surface site ratios for each model set.

electron donor, aiming to provide insight into microstructure control of $MgCl_2$ crystallites with electron donors.

## 2. Computational details

Crystalline $MgCl_2$ exists in a sheet-like layered structure [37]. The models used in this study were cut out of a monolayer of β-$MgCl_2$ [37], the central atoms were frozen, and the coordinatively unsaturated surface magnesium atoms, together with the adjacent chlorines, were relaxed (see Fig. 2). Similar fixations were in effect on the models during the addition of methanol, whereby the surface atoms of the $(MgCl_2)_n$ crystallites and the donor molecules were relaxed and the central atoms frozen.

The $(MgCl_2)_n$ crystallites and the donor-saturated crystallites were optimized by the hybrid density functional B3LYP method in combination with the standard 6-31G* basis set. Additionally, in donor absorption studies, energies were calculated by a larger 6-311G** basis set to reduce errors arising from basis set superposition error. All calculations were carried out using the Gaussian 03 program package [38].

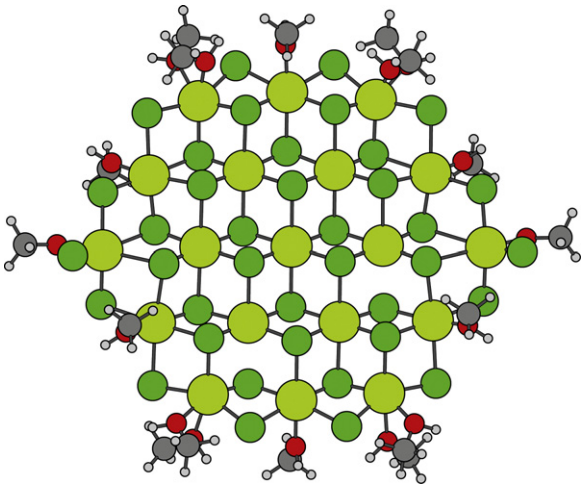

**Fig. 6.** Saturation of the $Mg_{19}Cl_{38}$ hexagon-shaped crystallite with methanol.

## 3. Results and discussion

### 3.1. The effects of shape and size on $MgCl_2$ crystallite stability

The effects of shape and size on the stability of $MgCl_2$ crystallites were studied using sets of differently shaped $(MgCl_2)_n$ models. The construction of each model set started with a small $(MgCl_2)_n$ crystallite ($n$ = 4–14), based on which the next member of the model set was obtained by systematically adding new $MgCl_2$ units. The model sets and the construction principle used for each model set are shown in Fig. 3. The initial structure is the smallest crystallite in each set, from which the next member of the set is derived by

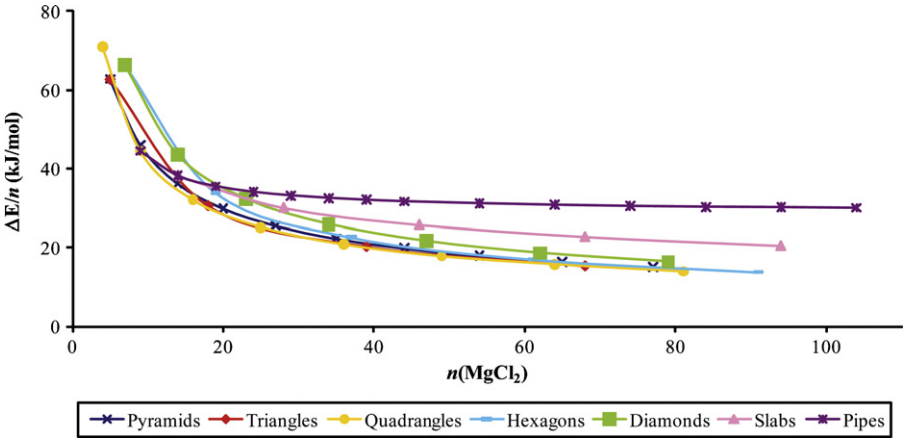


**Fig. 5.** The relative stabilities of the model sets in comparison to the infinite $MgCl_2$ sheet.

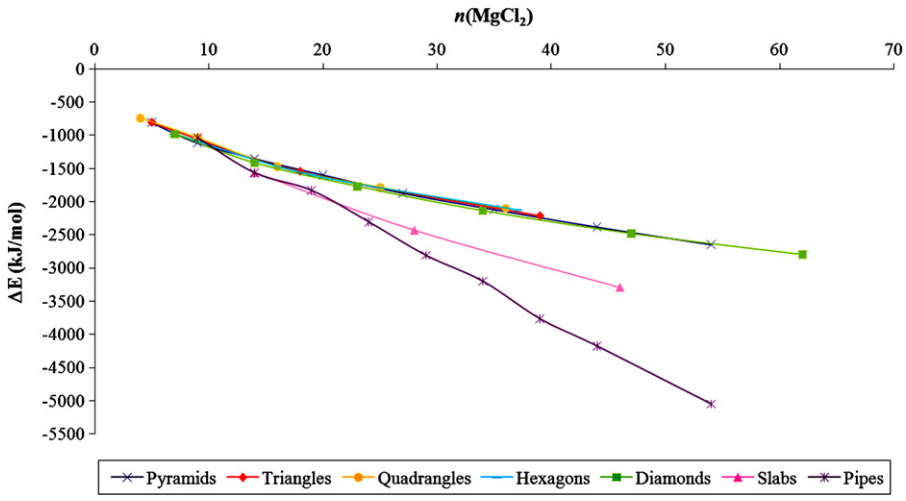


**Fig. 7.** Relative stabilities of the optimized donor-saturated crystallites.

adding $MgCl_2$ units as illustrated by the purple colored atoms in the enlarged models. The building-up process was repeated several times for each model set in order to obtain larger crystallites. The largest crystallites consist of up to one hundred $MgCl_2$ units, the dimensions of the crystallites ranging from approximately 0.5 nm to 13.5 nm in width. The model sets are named reflecting the shape of the crystallite.

Because the comparison of the (1 0 0) and (1 1 0) surface types of $MgCl_2$ was of specific interest, the model shapes were selected so that a dominance of either the (1 0 0) or the (1 1 0) surface sites over the other type exists in each model set. For the quadrangle, pyramid, triangle, diamond and hexagon shapes the ratio of (1 0 0) to (1 1 0) surface sites increases as the sizes of the crystallites are enlarged, making (1 0 0) the prevailing surface type in these model sets. For the slab and pipe models, on the other hand, the proportion of (1 1 0) surface sites increases as model size grows. Note that each shape necessarily contains both (1 0 0) and (1 1 0) surface sites in order to preserve the $MgCl_2$ stoichiometry. The (1 0 0) to (1 1 0) surface site ratios for the models are shown in Fig. 4.

The proportion of unsaturated edge magnesium atoms in the crystallite is another significant factor in determining crystallite stability. The model sets can be arranged in the following decreasing order according to the proportion of edge magnesium atoms: pipes, pyramids, quadrangles, triangles, diamonds, hexagons, and slabs.

The energies of the partly optimized $(MgCl_2)_n$ crystallites were compared to the energy of an infinite (0 0 1) β-$MgCl_2$ monolayer sheet. The relative stabilities divided by the number of $MgCl_2$ units ($\Delta E/n$) are shown in Fig. 5 for each model shape.

The relative stabilities of the crystallites approach the energy of the infinite $MgCl_2$ sheet as the size of the crystallites increases. As the size of the models grows, the crystallite starts to increasingly resemble the bulk $MgCl_2$ crystal lattice and the proportion of edge atoms decreases, leading to increased stability. Higher coordination numbers of the edge magnesium atoms is also a stabilizing factor, as the shapes rich in five-coordinated (1 0 0) surface sites are notably more stable than the slab and pipe models, in which the four-coordinated (1 1 0) surface sites prevail.

### 3.2. The effects of donor adsorption on $MgCl_2$ crystallite stability

The effects of electron donor adsorption on the stability order of the crystallite shapes were examined using methanol as the model donor. Methanol was selected as the model donor due to its simple and compact yet evidently electron-donating structure and the straightforward monodentate binding mode it exhibits on $MgCl_2$ surfaces. The surfaces were fully saturated by methanol, as depicted in Fig. 6 for the $Mg_{19}Cl_{38}$ hexagon-shaped crystallite.

The energies of the optimized donor-saturated $(MgCl_2)_n$ crystallites were compared to the energies of infinite $MgCl_2$ sheet and free methanol, resulting in the value of stabilization ($\Delta E$) caused by donor adsorption on the crystallite edges. $\Delta E$ was calculated according to Eq. (1), where the system means the optimized donor-saturated crystallite, $n$ is the number of $MgCl_2$ units and $m$ equals the number of added methanol molecules. The values of $\Delta E$ are plotted in Fig. 7 for each model set:

$$\Delta E = E(\text{system}) - nE(MgCl_2\ \text{sheet}) - mE(\text{MeOH}) \quad (1)$$

The adsorption of methanol on the crystallite edges has a distinct effect on the stabilities of the crystallites. The stability order for the largest crystallites is pipes > slabs > triangles > quadrangles > pyramids > diamonds > hexagons. The most intriguing difference in the stability order of the plain crystallites versus the donor-saturated crystallites is the respective change in the position of the pipe- and slab-shaped models from the least stable to the most stable crystallite shapes. This suggests that the (1 1 0) surface sites abundant in these model shapes are more effective in binding methanol than the (1 0 0) surface sites, leading to increased stabilization of the donor-saturated pipe models as opposed to for example the hexagon and diamond shapes, which following to donor addition are less stable than the pipe models. Excluding the pipe and slab models, the rest of the model sets more or less retain the same stability order as before donor addition.

## 4. Conclusions

The effects of crystallite shape and size on the stability of magnesium chloride crystallites were examined by quantum chemical calculations. Increasing crystallite size and the existence of high coordination numbers in the edge magnesium atoms emerged as factors enhancing crystallite stability. In particular, crystallite shapes with a high proportion of (1 0 0) surface sites as opposed to (1 1 0) surface sites have higher stability.

The crystallites were saturated with model donor methanol in order to study whether the stability order of the crystallite shapes can be affected with the inclusion of electron donors in the system. The addition of methanol greatly enhanced the stability of the (1 1 0) surface site rich crystallite shapes in comparison to the (1 0 0) surface site rich shapes. This indicates that the adsorption of methanol is more favorable on the (1 1 0) surface in compari-

son to the (1 0 0) surface of $MgCl_2$. With the choice of a suitable electron donor compound the formation of the (1 1 0) surface in $MgCl_2$ crystallites may therefore be favored over the (1 0 0) surface. The study providing a starting point, additional combined experimental and theoretical efforts will be necessary to establish the relationships between internal donors, catalyst microstructures and catalytic properties of the Ziegler–Natta catalysts.

## Appendix A. Supplementary data

Supplementary data associated with this article can be found, in the online version, at doi:10.1016/j.molcata.2010.11.003.

## References


[1] N. Kashiwa, J. Polym. Sci. A: Polym. Chem. 270 (2007) 164.
[2] W. Kaminsky, M. Arndt, Handbook of Heterogeneous Catalysis, vol. 5, first ed., VCH, Weinheim, 1997, p. 2405 (and refs. therein).
[3] J.J.A. Dusseault, C.C. Hsu, Rev. Macromol. Chem. Phys. 33 (1993) 103.
[4] D.A. Trubitsyn, V.A. Zakharov, I.I. Zakharov, J. Mol. Catal. A: Chem. 270 (2007) 164.
[5] U. Giannini, Makromol. Chem. Suppl. 5 (1981) 261.
[6] P. Corradini, V. Barone, R. Fusco, Guerra, Gzz. Chim. Ital. 113 (1983) 601.
[7] E. Albizzati, M. Galimberti, U. Giannini, G. Morini, Makromol. Chem. Macromol. Symp. 48/49 (1991) 223 (and the refs. therein).
[8] V. Busico, M. Causa, R. Cipullo, R. Credendino, F. Cutillo, N. Friederichs, R. Lamanna, A. Segre, V. Castelli, J. Phys. Chem. C 112 (2008) 1081.
[9] G. Monaco, M. Toto, G. Guerra, P. Corradini, L. Cavallo, Macromolecules 33 (2000) 8953.
[10] M. Toto, G. Morini, G. Guerra, P. Corradini, L. Cavallo, Macromolecules 33 (2000) 1134.
[11] T. Taniike, M. Terano, Macromol. Symp. 260 (2007) 98.
[12] T. Taniike, M. Terano, Macromol. Rapid Commun. 28 (2007) 1918.
[13] T. Taniike, M. Terano, Macromol. Rapid Commun. 29 (2008) 1472.
[14] J.S. Lin, C.R.A. Catlow, J. Catal. 157 (1995) 145.
[15] J.D. Gale, C.R.A. Catlow, M.J. Gillan, Top. Catal. 9 (1999) 235.
[16] H. Weiss, M. Boero, M. Parrinello, Macromol. Symp. 173 (2001) 137.
[17] E. Puhakka, T.T. Pakkanen, T.A. Pakkanen, J. Phys. Chem. A 101 (1997) 6063.
[18] L. Brambilla, G. Zerbi, S. Nascetti, F. Piemontesi, G. Morini, Macromol. Symp. 213 (2004) 287.
[19] L. Brambilla, G. Zerbi, F. Piemontesi, S. Nascetti, G. Morini, J. Mol. Catal. A Chem. 263 (2007) 103.
[20] J.C. Chadwick, Macromol. Symp. 173 (2001) 21 (and the refs. therein).
[21] E. Albizzati, U. Giannini, G. Morini, M. Galimberti, L. Barino, R. Scordamaglia, Macromol. Symp. 89 (1995) 73 (and the refs. therein).
[22] L. Barino, R. Scordamaglia, Macromol. Symp. 89 (1995) 101.
[23] G. Morini, E. Albizzati, G. Balbontin, I. Mingozzi, M.C. Sacchi, F. Forlini, I. Tritto, Macromolecules 29 (1996) 5770.
[24] L. Barino, R. Scordamaglia, Macromol. Theory Simul. 7 (1998) 399.
[25] S. Yao, Y. Tanaka, Macromol. Theory Simul. 10 (2001) 850.
[26] A. Andoni, J.C. Chadwick, S. Milani, H.J.W. Niemantsverdriet, P.C. Thüne, J. Catal. 247 (2007) 129.
[27] A. Andoni, J.C. Chadwick, S. Milani, H.J.W. Niemantsverdriet, P.C. Thüne, Macromol. Rapid Commun. 28 (2007) 1466.
[28] A. Andoni, J.C. Chadwick, S. Milani, H.J.W. Niemantsverdriet, P.C. Thüne, Macromol. Symp. 260 (2007) 140.
[29] A. Andoni, J.C. Chadwick, S. Milani, H.J.W. Niemantsverdriet, P.C. Thüne, J. Catal. 257 (2008) 81.
[30] D.V. Stukalov, V.A. Zakharov, I.L. Zilberberg, J. Phys. Chem. C 114 (2010) 429.
[31] S.B. Mukkamala, C.E. Anson, A.K. Powell, J. Inorg. Biochem. 100 (2006) 1128.
[32] H.G. Yang, C.H. Sun, S.Z. Qiao, J. Zou, G. Liu, S. Campbell Smith, H.M. Cheng, G.Q. Lu, Nature 453 (2008) 638.
[33] M. Seth, T. Ziegler, Macromolecules 36 (2003) 6613.
[34] V. Busico, P. Corradini, L. De Martino, A. Proto, V. Savino, E. Albizzati, Makromol. Chem. 186 (1985) 1279.
[35] D.V. Stukalov, V.A. Zakharov, A.G. Potapov, G.D. Bukatov, J. Catal. 266 (2009) 39.
[36] K. Vanka, G. Singh, D. Iyer, V.K. Gupta, J. Phys. Chem. C 114 (2010) 15771.
[37] I.W. Bassi, F. Polato, M. Calcaterra, J.C.J. Bart, Z. Kristallogr. 159 (1982) 297.
[38] M.J. Frisch, G.W. Trucks, H.B. Schlegel, G.E. Scuseria, M.A. Rob, J.R. Cheeseman, J.A. Montgomery Jr., T. Vreven, K.N. Kudin, J.C. Burant, J.M. Millam, S.S. Iyengar, J. Tomasi, V. Barone, B. Mennucci, M. Cossi, G. Scalmani, N. Rega, G.A. Petersson, H. Nakatsuji, M. Hada, M. Ehara, K. Toyota, R. Fukuda, J. Hasegawa, M. Ishida, T. Nakajima, Y. Honda, O. Kitao, H. Nakai, M. Klene, X. Li, J.E. Knox, H.P. Hratchian, J.B. Cross, V. Bakken, C. Adamo, J. Jaramillo, R. Gomperts, R.E. Stratmann, O. Yazyev, A.J. Austin, R. Cammi, C. Pomelli, J.W. Ochterski, P.Y. Ayala, K. Morokuma, G.A. Voth, P. Salvador, J.J. Dannenberg, V.G. Zakrzewski, S. Dapprich, A.D. Daniels, M.C. Strain, O. Farkas, D.K. Malick, A.D. Rabuck, K. Raghavachari, J.B. Foresman, J.V. Ortiz, Q. Cui, A.G. Baboul, S. Clifford, J. Cioslowski, B.B. Stefanov, G. Liu, A. Liashenko, P. Piskorz, I. Komaromi, R.L. Martin, D.J. Fox, T. Keith, M.A. Al-Laham, C.Y. Peng, A. Nanayakkara, M. Challacombe, P.M.W. Gill, B. Johnson, W. Chen, M.W. Wong, C. Gonzalez, J.A. Pople, Gaussian 03, Revision C.02, Gaussian, Inc., Wallingford, CT, 2004.